Heat Transfer and Unsaturated Flow Phenomena in Rigid Dual-Scale Porous Media

Nirmal Kumar Balaguru[1], M. Jeyameena[2]

[1]Development Engineer, Kraft Recovery Boilers (R&D), Andritz paper and pulp
[2]Student, Hindusthan College of Engineering and Technology, Coimbatore

Abstract— *Composites are light weighted materials that can replace the metals in strength promisingly in future. The residual porosity of the composites alters the thermo-physical properties of the material to a maximum level. During the impregnation of fibre in matrix (injection), the presence of air voids changes the direction of the flow of resin. This also affects the material properties in terms of flexibility, durability but agitates the effective thermal conductivity (k_{eff}).The physics behind the effect of air void on the effective thermal conductivity cannot be captured in commercial software or experiments. The best way to solve this problem is by numerical codes using finite element approach, by dividing the whole macroscopic domain into numerous subdomains as possible. The divided subdomain should be periodic in nature with respect to the whole domain. If the heterogeneities are similar, dual scale approach is used and so on. If the heterogeneities are different and if they are of two types, triple scale approach is used. The contrast ratio and volume percentage of fiber is used as variables. The air void creates a giant leap for saturation in both, which in turn effect the effective thermal conductivity. Air void troubles the effective thermal conductivity mainly because of its insignificance in scalar values of thermal conductivity when it is compared to fiber or matrix mathematically.*

Keywords— *composites, effective thermal conductivity, homogenization, impregnation, matrix, fibre, preform, contrast ratio, saturation, liquid composite moulding.*

I. INTRODUCTION

The Liquid Composite moulding (LCM) is one of the most predominant processes in the manufacturing of composites. The reinforcement of dry fiber called as perform is kept inside the moulding cavity. The moulding cavity is locked and the resin is injected to the moulding cavity. Initially, the resin that is injected to moulding cavity will rush the air entrapped between the fibrous networks outside the moulding cavity thus forming a composite on curing.

The major defect during injection is voids, These are due to entrapment of dissolved volatile gases in resin or due to improper balance of velocity and capillary force. There are voids formed within the tows and also in between the tows, naming micro porosity and macro porosity respectively. As described by R.J Bascom [1],the composite test rings having void contents of 0.2 Volume % or less had interlaminar shear strengths 40-100% greater than the conventional rings with high void contents(5%).The void formation is related to the liquid properties and fluid-liquid contact angle. The micro scale flow pattern and the void formation, movement and removal is related to fibre mat architecture [7].

The laminates with the highest average content of voids had an transverse strain to failure as high as 2% whereas low void content laminates failed at 0.3%. Low void content laminates form only few large and well defined transverse cracks whereas the high void content laminates form multiple transverse cracks with irregular shapes and also small cracks. The irregularity of these cracks results in lower stress concentration as per the conclusion of J.Vama [2].

The LCM processes such as Resin transfer moulding is increasingly used to manufacture parts of industrial application and were cost efficient. The work by LS Lecrec [5] which was carried out on different type of fibrous reinforcements and the optimal condition for the impregnation of resin to avoid macro and micro voids relating the local capillary number. The contrasts in the thermal properties existing between the dry and the fully saturated reinforcement is used to determine the dynamic saturation curve. As explained by Maxime Viliere [6] the evolution of residual voids for several resin flow rates with respect to the capillary number.

When the material properties of the composites are known the effective thermal conductivities of woven-reinforcement composites is predicted the models proposed by Maxime Villiere [9].The heterogeneous media uses two pairs of local and

homogenized problems, described at the smallest scale is seen to affect the medium macro-scale or effective behaviour. The homogenization is used to formulate the Fourier heat conduction problem[10].The homogenization process using the double scale asymptotic developments as macroscale and microscale is much appropriate[11] and it also permits the determination of the correct model for a given macroscopic boundary value [12].

II. METHODOLOGY

2.1 Homogenization

This process can be defined as the converting the domain with numerous heterogeneities to homogeneous domain. It is a process in which the heterogeneities in a domain are divided into small subdomain. This process can be defined as the converting the domain with numerous heterogeneities to equivalent homogeneous domain. Consider heat equation,

$$\rho C_p \frac{\partial T}{\partial t} + div\,.\,(K.\nabla T) = 0 \tag{1}$$

Assuming it as steady heat flux,

$$div\left(-\varphi\right) = 0 \tag{2}$$

Where $\emptyset$ is the heat flux density

$$\varphi = K.\nabla T \tag{3}$$

The version of homogenised equation can be written as

$$<\varphi> = <\varphi(X).\nabla T\,(X)> = K^*.<\nabla T> \tag{4}$$

Where k* is known as effective thermal conductivity in macroscopic scale. We can see how the conductivity in the micro scale is homogenised to macro scale through the process of homogenisation.

2.1.1 Analytical Method

Consider a domain Ω, having the boundary $\partial\Omega$. The microscopic domain surfaces are periodic which means that the same domain can be repeated numerous times as required. The borders of the domain are having the temperature of T^0 .
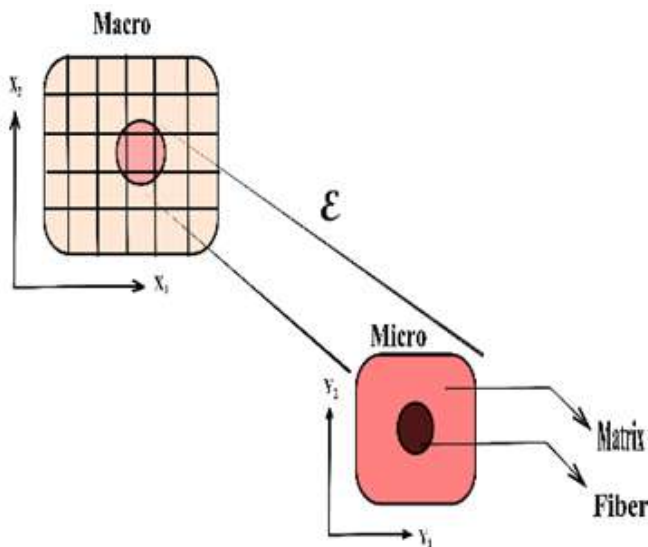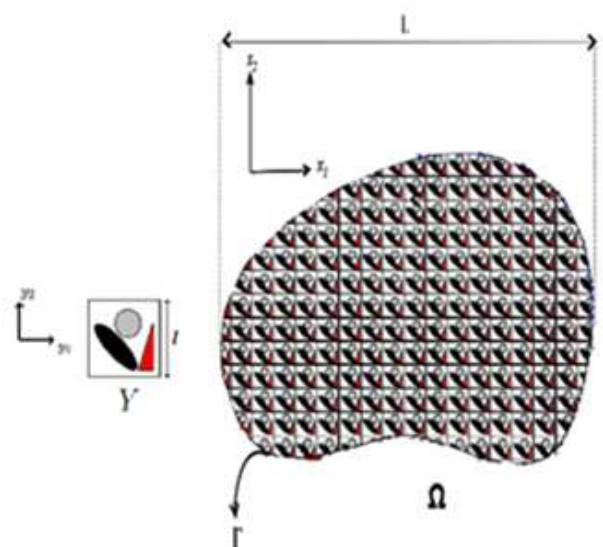

FIG 1: Physical way of Homogenization   FIG 2: Micro and Macro cells

$$div_X\left(-\emptyset^\varepsilon(X)\right) = f(x) \qquad in\ \Omega \tag{5}$$

$$\emptyset^\varepsilon(X) = K.\nabla_X T^\varepsilon\,(X) \qquad in\ \Omega \tag{6}$$
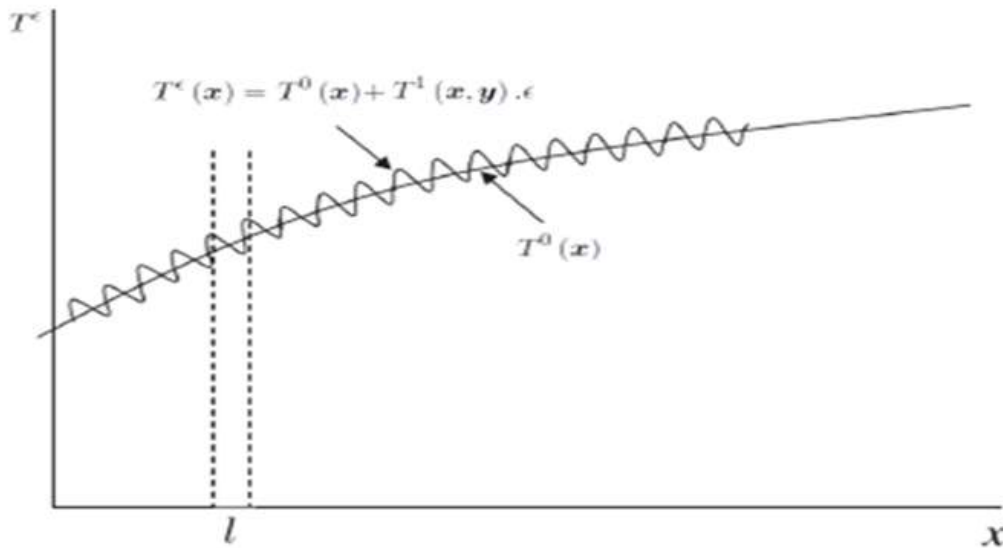
$$T = T^0 \qquad on\ F \tag{7}$$

FIG 3: Asymptotical approach

To determine the asymptotic behaviour of the temperature T and flux Ø, solutions of the heterogeneous problem arises when ε tends to 0 when we use here the method asymptotic developments several scales. This is done by expanding T by the following development.

$$T^\varepsilon(x,y) = T^0(x,y) + \varepsilon T^1 + \varepsilon^2 T^2 + .. \tag{8}$$

$$\emptyset^\varepsilon(x,y) = \emptyset^0(x,y) + \varepsilon\emptyset^1 + \varepsilon^2\emptyset^2 + ... \tag{9}$$

Divergence between macro and micro scales can be derived as,

$$\nabla = \frac{\partial}{\partial x} + \frac{1}{\varepsilon} + \frac{\partial}{\partial y} \tag{10}$$

When the divergence are expanded in heat equation for k, T and T is expanded asymptotically, Steady state heat conduction equation

$$\nabla.(K \nabla T) = 0 \tag{11}$$

solving for ε^{-2} problem it leads to, $T^0 \rightarrow T(x)$ only Hence T^0 can be only usedfor macroscale.

solving for ε^{-1} problem it leads to,

$$T^1(x,y) = W.\nabla.T^0 \tag{12}$$

And also the cell equation

$$\nabla_y\left(K\left(e_i + \nabla_y W_i\right)\right) = 0 \tag{13}$$

Solving for ε^0 problem it leads to,

$$\nabla_X[\frac{1}{|P|}\int_p K\left(I + \nabla_y W(y)\right)] \nabla_X T^0 = 0 \tag{14}$$

And

$$K^* = \frac{1}{|P|}\int_p K\left(I + \nabla_y W(y)\right) \tag{15}$$

such that

$$\nabla K \nabla T = 0$$
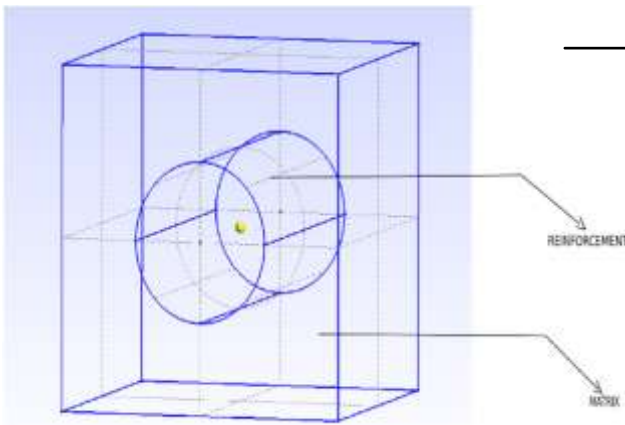
2.1.2   Numerical Analysis

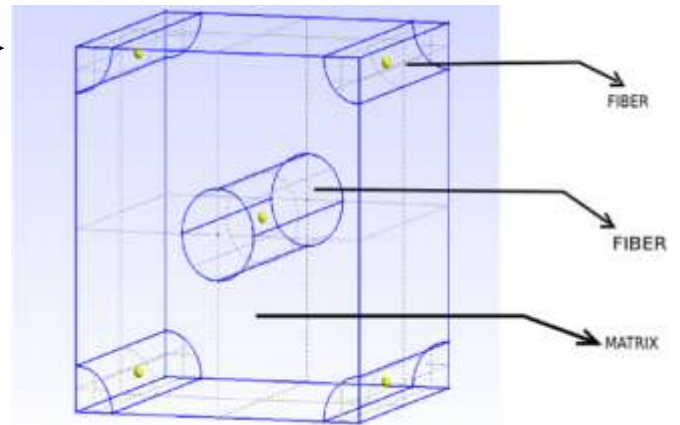**FIG 4: Type 1 cell – fiber at centre alone**   **FIG 5: Type 2 cell – fiber at centre and at corner**

The unit cell geometry is created by having fiber at centre alone and fiber with centre and at corner also. Since, it is a unit cell the cube is of dimensions 1 x 1 x 1. The Grid independence study has been carried out for three different characteristic length and the k_{eff} has found the minimum change between the two types.

The characteristic element doesn't have any length since, it is dimensionless. Gmsh software is used to generate the geometry and mesh and the Free Fem++ is used to solve the problem.

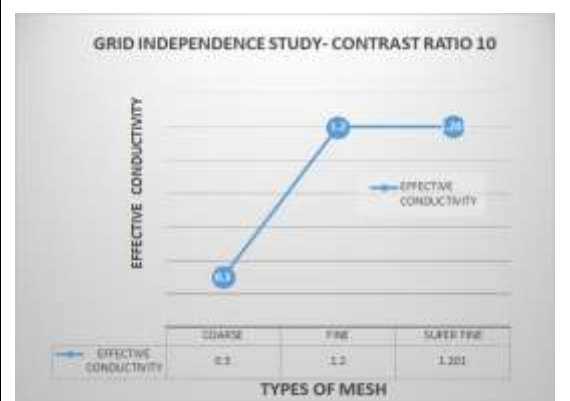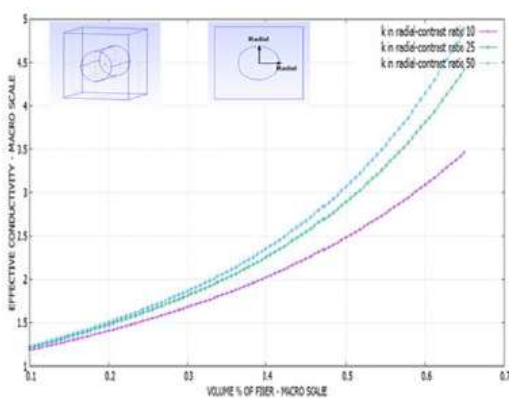|	**COARSE**	**FINE**	**SUPER-FINE**	
VERTICES	1237	10081	69481	
TETRAHEDRONS	4672	54272	384176	
TRIANGLES	1728	4096	15384	
No of ELEMENTS	6400	58368	350560	
FIG 6 & 7: Grid Independence study				

FIG 8: The evolution of k_{eff} at macroscale in radial direction with different C.R
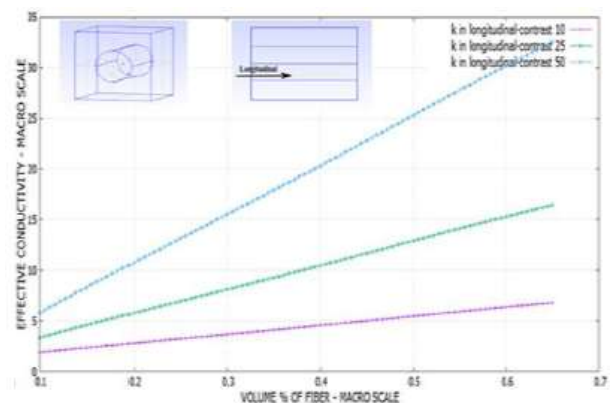

FIG 9: The evolution of k_{eff} at macroscale in longitudinal direction with different C.R.
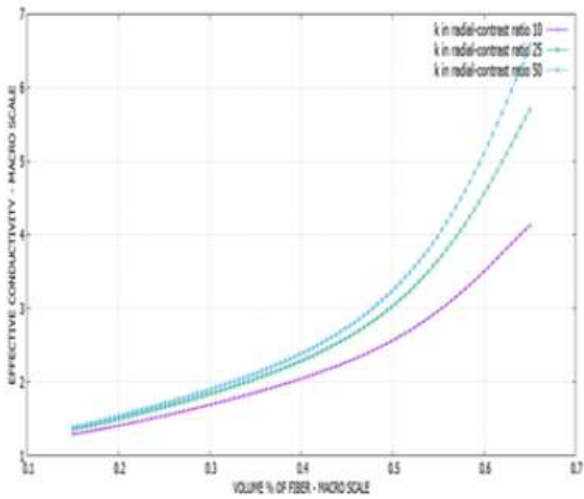
FIG 10: The evolution of k$_{eff}$ at macroscale in radial direction with different C.R – Type 2 cell
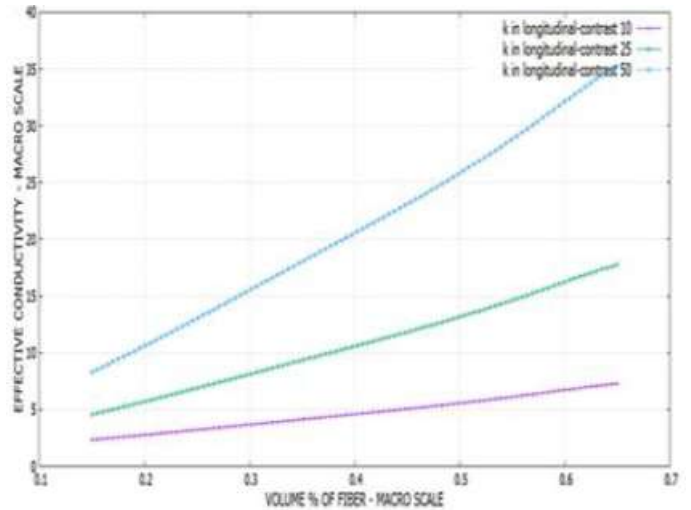

FIG 11: The evolution of k$_{eff}$ at macroscale in longitudinal direction with different C.R – Type 2 cell
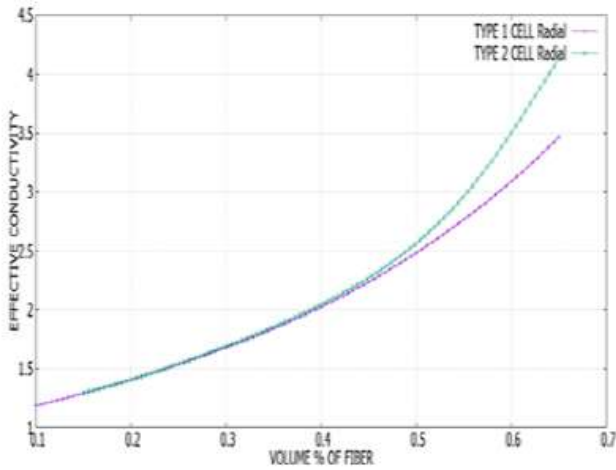

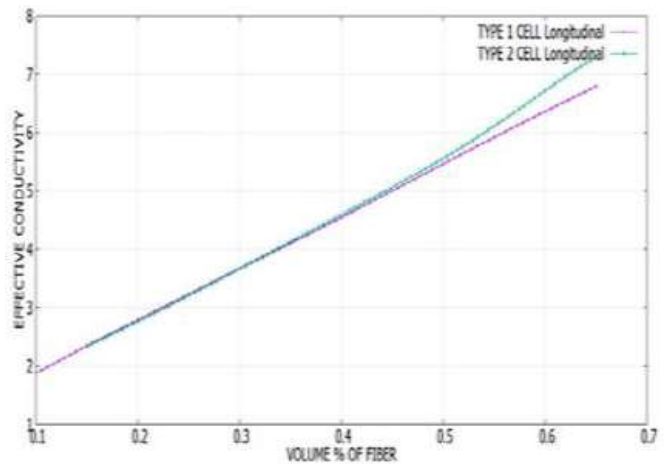**FIG 12: Type 1 Vs Type 2 cell in radial direction for contrast ratio 10**

FIG 13: Type 1 Vs Type 2 cell in longitudinal direction for contrast ratio 10

2.2   Triple Scale

In the iterative homogenization, the homogenization is done multiple times in which the solution of microscopic scale to mesoscopic tows are taken. On preceding the next step of homogenization the macroscopic properties are obtained.
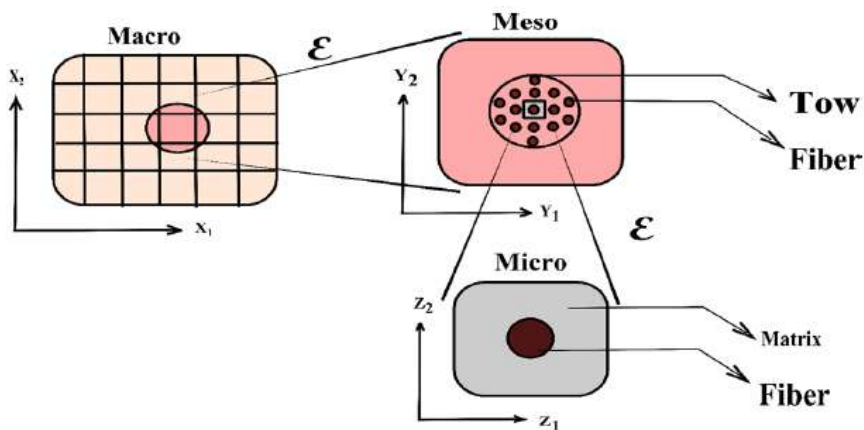

FIG 14: Iterative Homogenisation

2.2.1   Analytical Analysis

If the heterogeneities are in dual scale, homogenisation is done in iterative manner. This can be considered as a realistic approach.

The macro, meso and micro scale is taken as x, y and z scale respectively. The divergence in x,y,z scales are differentiated as,

$$\nabla_x = \begin{pmatrix} \frac{\partial}{\partial x_1} \\ \frac{\partial}{\partial x_2} \\ \frac{\partial}{\partial x_3} \end{pmatrix} \nabla_y = \begin{pmatrix} \frac{\partial}{\partial y_1} \\ \frac{\partial}{\partial y_2} \\ \frac{\partial}{\partial y_3} \end{pmatrix} \nabla_z = \begin{pmatrix} \frac{\partial}{\partial z_1} \\ \frac{\partial}{\partial z_2} \\ \frac{\partial}{\partial z_3} \end{pmatrix} \tag{17}$$

The calculation can be done with

$$\nabla = \frac{\partial}{\partial x} + \frac{1}{(\varepsilon)} \frac{\partial}{\partial y} + \frac{1}{(\varepsilon^2)} \frac{\partial}{\partial z} \tag{18}$$

When this is substituted to heat equation,

$$\nabla \cdot (K \nabla T) = 0 \tag{19}$$

The equations which we obtain are similar, but the only difference is calculation is carried in two steps. Micro   meso is one step and meso macro is another step.

As a first step let us explain T^ε

$$T^\varepsilon(x, y) = T^0(x, y) + \varepsilon T^1 + \varepsilon^2 T^2 + \dots \tag{20}$$

The divergence between meso and micro scales can be declared as

$$\nabla = \frac{\partial}{\partial y} + \frac{1}{\varepsilon} \frac{\partial}{\partial z} \tag{21}$$

When it is solved for $\nabla k \nabla T$, by taking mean and applying greens theorem for order -2 we will get to know that T^0 is a macroscopic property

When we solve the order of -1 we will get cell equation as,

$$\nabla_z (k(e_i + \nabla_z W_i) = 0 \tag{22}$$

And also the same order of scaling factor leads to

$$T^1 \rightarrow T^1(x, y) = X(y) \cdot \nabla_x T^0 \tag{23}$$

The effective conductivity in radial and longitudinal direction for micro scale is found using the following equation. These values are substituted to effective conductivities for meso scale and so the macro properties are found

$$k^* = \frac{1}{|p|} \int_p k \left(I + \nabla_y W(y) \right) dp \tag{24}$$

The same procedure has to be carried out for the meso macro where the macro properties are found

$$k^* = \frac{1}{|p|} \int_p k \left(I + \nabla_x X(y) \right) dp \tag{25}$$

Where P refers to the periodic domain. So the thermal conductivities obtained in this meso scale is considered as the final values for the macro scale.

2.2.2   Numerical analysis

Iterative homogenisation in actual: The cell geometry used for microscopic scale and mesoscopic scale should be different. The double homogenisation method should be more realistic. An elliptical geometry is considered in mesoscopic scale and the similar cylinder geometry is carried out for microscopic scale. This is a true approach and can be used for better accuracy. The microscopic heterogeneities repeat periodically in mesoscopic scale and mesoscopic heterogeneities are repeating periodically in macroscopic scale.
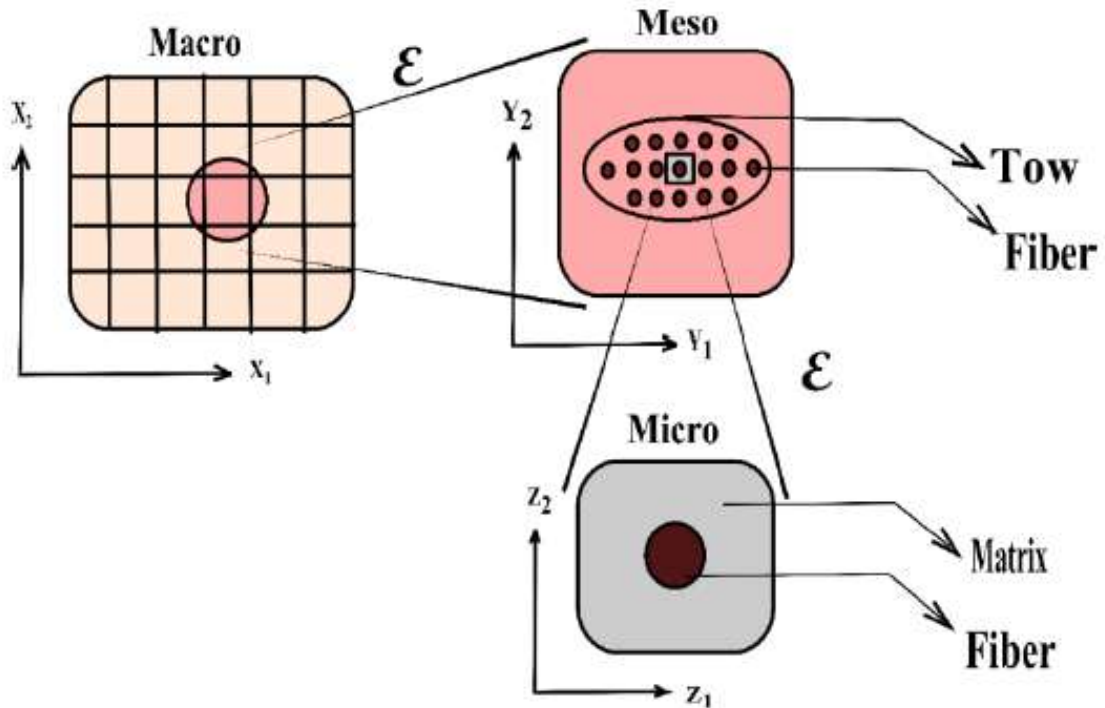
FIG 15: Physical explanation for actual way to do double

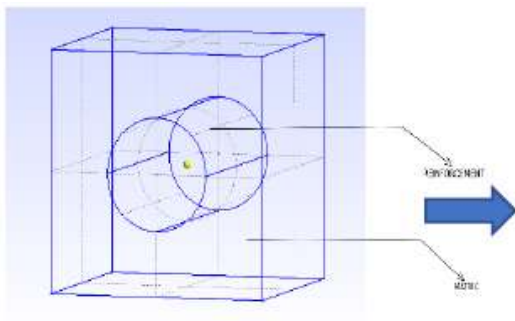This is done using software as follows when we implement to the unit cell with fibre in centre alone.

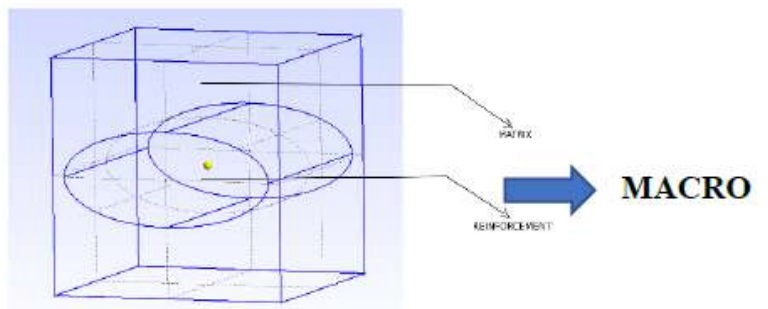| **FIG 16: Micro cell for actual double homogenisation** | **FIG 17: Meso cell for actual double homogenisation** |

The evolution in meso scale

10%of tow content   40% of tow content content   65% of tow content content
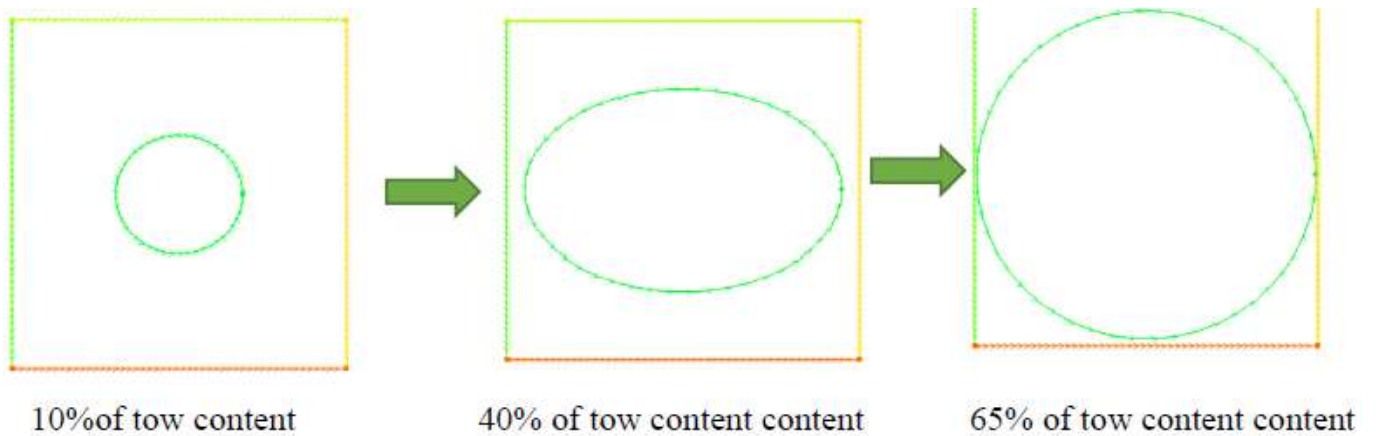
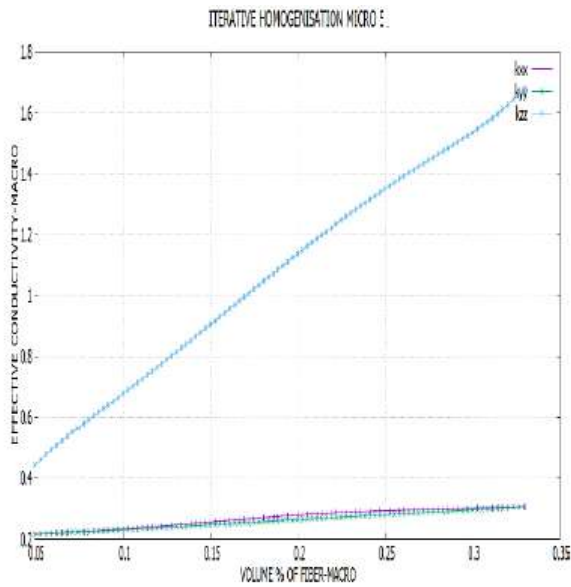**FIG 18: Evolution of Meso scale**

FIG 19: Effective conductivity in radial and longitudinal direction for volume percentage of fiber in micro scale is fixed to 65
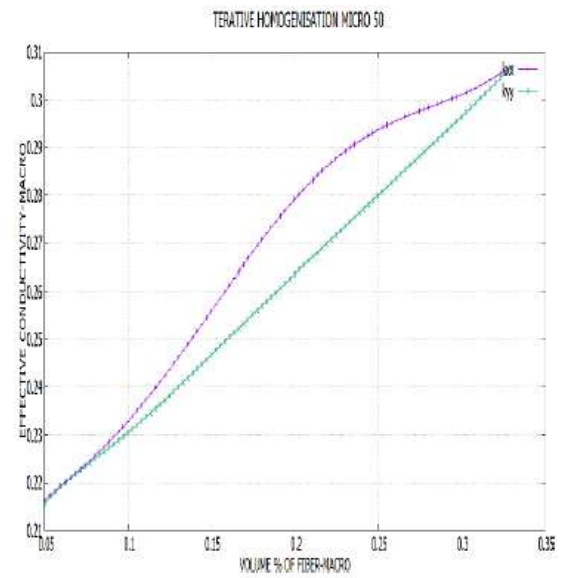
FIG 20: Zoomed view for plot to explain effective conductivity in radial direction

When the fiber inside the microscopic unit cell is fixed as 50% for whole cell volume, and if the fiber inside the mesoscopic cell is changed from 10% to 65 % the following plot is obtained. Plots to explain effective conductivity in radial and longitudinal direction for volume percentage of fiber in micro scale is fixed to 65. Zoomed view for plots to explain effective conductivity in radial direction.

2.3 Saturation

The voids created in LCM are of different natures depending on whether they are in or between the fibre it can lead to two effects micro-saturation, macro-saturation. The geometric parameters are of the two scales reinforcement. The volume rate of fibres in the composite is noted as φ_f^c. The volume percentage of fibre in microscale denoted by φ_f^m. The volume fraction in a tow is φ_m^c.

Such that

$$\varphi_f^c = \varphi_f^m * \varphi_m^c \tag{2.26}$$

2.3.1 Micro saturation

Micro saturation is defined as the space that is present in the cell for the matrix to fill in Micro Scale. Micro-saturation is calculated as followed,

$$S\mu = 1 - \frac{volume\ percentage\ of\ airvoid\ in\ microscale}{volume\ percentage\ of\ matrix\ in\ microscale}$$
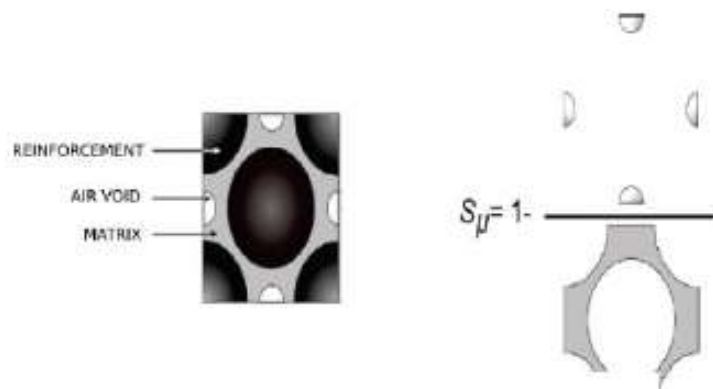

FIG 21: Micro saturation

2.3.2   Micro saturation

Macro-saturation is defined as the complement of the ratio of the total volume of macro voids subtracted to the total volume they could take maximum, namely the inter-space available other that bubbles.
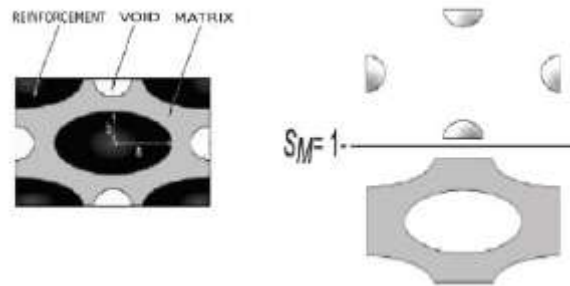

FIG 22: Meso Saturation

$$SM = 1 - \frac{volume\ percentage\ of\ airvoid\ in\ macroscale}{volume\ percentage\ of\ matrix\ in\ macroscale}$$

2.3.3   Total saturation

The total saturation or the overall saturation of the reinforcement as a linear combination of micro- and macro-saturations, weighted by factors that depend only on the geometry of the fiber and voids. These reflect the fluid fractions present in the strands and between the strands.

The Total saturation is obtained by

$$S_T = \left(\frac{\varphi_m^c - \varphi_f^c}{1 - \varphi_f^c}\right)S_\mu + \left(\frac{1 - \varphi_m^c}{1 - \varphi_f^c}\right)S_M? \tag{27}$$
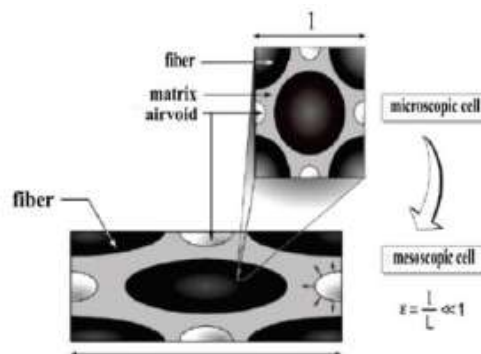

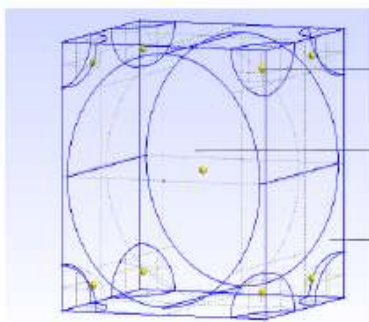**FIG 23: Iterative homogenization**

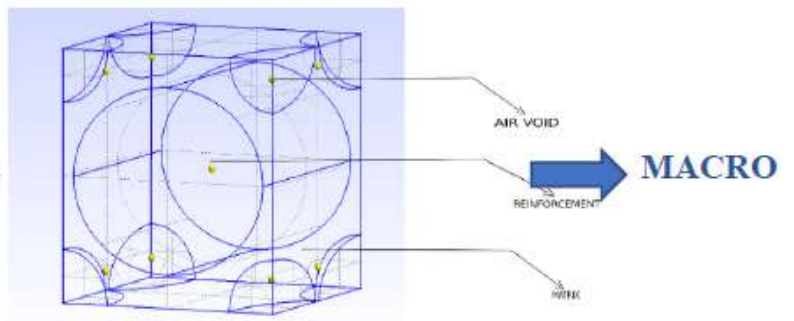**FIG 24: Micro cell with voids**   **FIG 25: Meso cell with voids**

Where $S_M = 0$ the curve is obtained, the space intermeches is filled in an ideal manner, the bubbles located only within the stands. The above tells us that the inter-locks space represent 59% of the volume that can occupy the fluid because

$$\left(\frac{1-\varphi_m^c}{1-\varphi_f^c}\right) = 0.59 \tag{28}$$

Calculation of the thermal conductivity was then repeated for all possible pairs of Sµ-SM. The curves are set in SM, and for each value of Sµ, the ST value is found. The set of curves obtained represents what is referred to hereinafter as a set of curves radial and longitudinal thermal conductivity.

2.4   Computational method

The calculations are done by fixing the saturation in meso scale, and changing the saturation value in micro scale from 1 that is known as fully saturated to 0 where only dry air is present.

The values of effective conductivity that are obtained are plotted against the total saturation values

TABLE 1
PARAMETERS FOR STUDY SATURATION

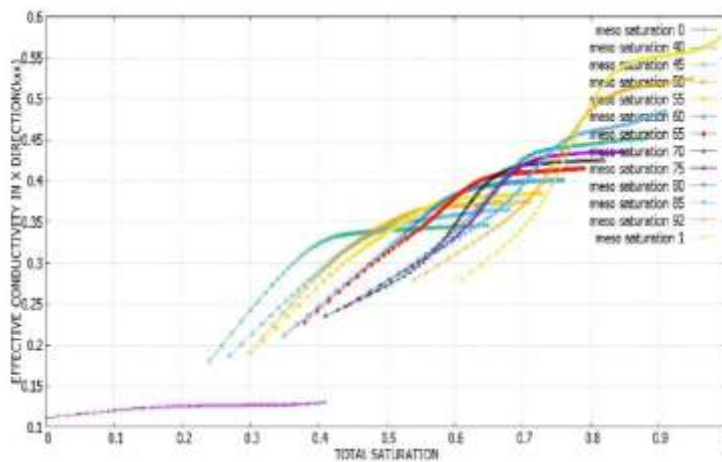| Parameters	Values
φ_m^c	0.70
φ_f^c	0.70
φ_f^c	0.49
rf	0.472
a	0.45
b	0.37

FIG 26: Plot that explains about variation of effective conductivity in x – direction w.r.t. total saturation
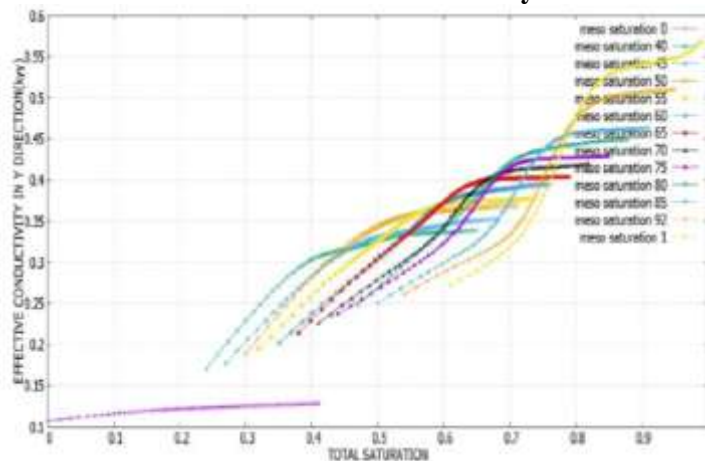

FIG 27: Plot that explains about variation of effective conductivity in y – direction w.r.t. total saturation
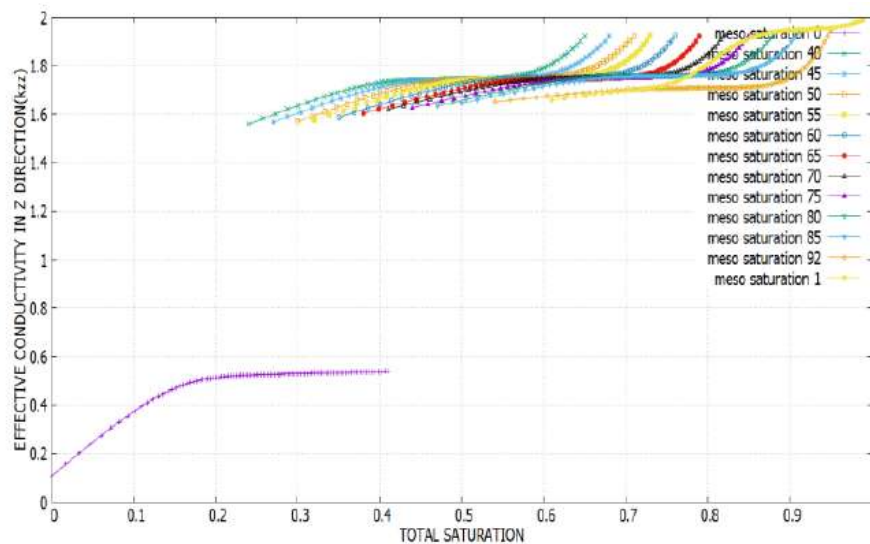
FIG 28: Plot that explains about variation of effective conductivity in y – direction w.r.t. total saturation

III.　CONCLUSION

By this research work the following studies had been done.

- The contrast ratio influences effective thermal conductivity. The ratio of thermal conductivity between the fibre and matrix is known as contrast ratio. As this parameter increases the effective thermal conductivity increases drastically.

- The volume percentage of fibre in macro scale can be determined directly by the fibre content in micro scale in dual homogenisation. In iterative homogenisation the volume percentage of fibre in macro scale is determined by fibre content in micro scale and the rate at which fibre is rooved.

- The effective thermal conductivity depends on the position and shape of the fibre. As the volume percentage of fibre increases, the effective conductivity increases gradually in radial direction and increases linearly (most likely) in longitudinal direction.

- The iterative homogenisation is most useful for realistic approach since the geometry of fibre in micro scale differs with the geometry of tow in the mesoscale. This method increases the accuracy in terms of volume percentage of fibre.

- The micro and macro voids effects micro and meso saturation. The effective conductivity decreases when the saturation decreases or the volume occupied by the air void increases

REFERENCES

[1] R. J. Bascom WDD, ",.Microvoids in glass resins composites:their origin and effect on composite strength," Ind Eng Chem Prod Res Dev, pp. 7(3):172-8., 1968.

[2] J. R. B. L. L. T. Varna J, " Effect of voids on failure machanisms laminates in RTM laminates," Compos Sci Technol , pp. 53:241-9., 1995.

[3] L. A. S. A. B. J. l. L. W. Park CH, " Modeling and simulation of voids and saturation liquid composite moulding process," Compos Part A: Appl Sci Manuf , pp. 42(6):658-68., 2011.

[4] G. B. L. C. Lundstrom TS, " Void formation in RTM.," J. Reinf. Plast. Compos., pp. 12(12):1339-49. , 1993.

[5] R. E. Lecrec JS, "Porosity reduction using optimized flow velocity in resin transfer mouding," Compos Part A: Appl Sci Manuf , pp. 39(12):1859-69., 2008.

[6] S. G. V. S. N. B. J. B. D. D. Maxime Villiere, "Dynamic saturation curve measurement in liquid composite moulding by heat transfer analysis.," Compos Part A, pp. 69:255-265, 2015.

[7] N. P. a. LEE, " Effect of Fiber Mat Architecture on void formation and removal in LCM.," Polymer compos, pp. 16(5): 386-399., 1995.

[8] A. S. T. S. W. a. S. A. RS Parnas, " The interactions between Microscopic and Macroscopic flow in RTM preforms.," Compos Struct, pp. 27:93-107., 1994.

[9]   D. L. V. S. N. B. D. D. M.Villiere, "Experimental Determination and modelling thermal conductivity tensor of carbon/epoxy composite.," Compos Part A, pp. 46:60-68, 2012.

[10] M. E. C. a. J. B. C. E. I. Rodriguez, "Reiterated homogenisation applied to heat conduction in heterogenous media with multiple spatial scales and perfect thermal contact between phases," J Braz Soc Mech Sci Eng, no. 10.1..7/s40430-016-0497-7.

[11] J. L. Auriault, "Heterogenous medium is an equivalent macroscopic description is possible," Int. J. Engg , vol. 29, pp. 7:785-795 , 1991.

[12] J. L. A. a. H. I. ENE, "Macroscopic modelling of heat transfer in composites with interfacial thermal barrier," Int. J. Engg , vol. 37, no. 18, pp. 2885-2892., 1994.

[13] C.-Y. W. a. C. Beckermann, "A two-Phase mixture model of liquid – gas flow and heat transfer in capillary porous media-I formulation," Int. J. HMT, vol. 36, no. 11, pp. 2747-2758, 1993.

[14] L. D. S. L. C. a. J. A. J P Vassal, "Upscalling the diffusion equations in particulate media made of highly conductive particles," American Physical Theory, no. 1539-3755/2008/77(1)/011302(10)., 2008.

[15] M. Kaminski, "Homogenisation of Transient Heat Transfer Problems for Some Composite Materials," Int. J. Engg. Sci, no. 41, pp. 1-29, 2003.

[16] M. Kaviany., Principles of Heat Transfer in Porous media, Michigan: springer, 1999.